HHS Public Access

Author manuscript

Mol Cell. Author manuscript; available in PMC 2016 July 16.

Published in final edited form as:

Mol Cell. 2015 July 16; 59(2): 298–308. doi:10.1016/j.molcel.2015.06.011.

Glutaminolysis and Transferrin Regulate Ferroptosis

Minghui Gao[1], **Prashant Monian**[1], **Nosirudeen Quadri**[2], **Ravichandran Ramasamy**[2], and **Xuejun Jiang**[1]

[1]Cell Biology Program, Memorial Sloan-Kettering Cancer Center, 1275 York Avenue, New York, NY 10065, USA

[2]Department of Medicine, Langone Medical Center, New York University, 522 1st Avenue, New York, NY 10016, USA

SUMMARY

Ferroptosis has emerged as a new form of regulated necrosis that is implicated in various human diseases. However, the mechanisms of ferroptosis are not well defined. This study reports the discovery of multiple molecular components of ferroptosis and its intimate interplay with cellular metabolism and redox machinery. Nutrient starvation often leads to sporadic apoptosis. Strikingly, we found that upon deprivation of amino acids, a more rapid and potent necrosis process can be induced in a serum-dependent manner, which was subsequently determined to be ferroptosis. Two serum factors, the iron-carrier protein transferrin and amino acid glutamine, were identified as the inducers of ferroptosis. We further found that the cell surface transferrin receptor and the glutamine-fueled intracellular metabolic pathway, glutaminolysis, played crucial roles in the death process. Inhibition of glutaminolysis, the essential component of ferroptosis, can reduce heart injury triggered by ischemia-reperfusion, suggesting a potential therapeutic approach for treating related diseases.

Graphical Abstract

To whom correspondence should be addressed: Xuejun Jiang, jiangx@mskcc.org.

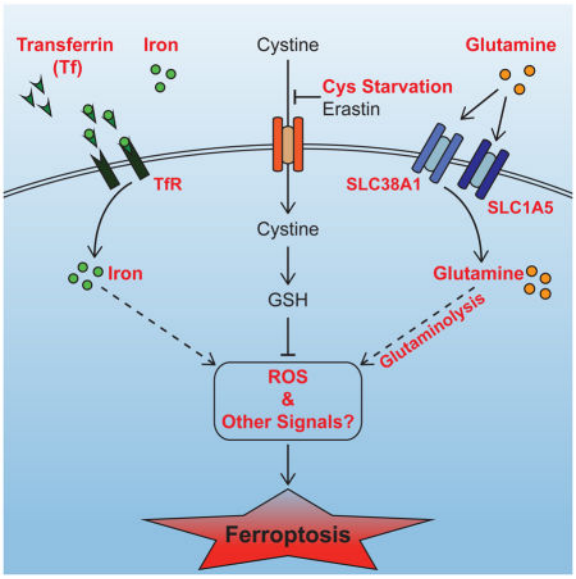

INTRODUCTION

In multicellular organisms, programmed cell death, particularly apoptosis, is frequently activated in a highly orchestrated manner to fulfill specific physiological functions (Budihardjo et al., 1999; Danial and Korsmeyer, 2004; Fuchs and Steller, 2011; Green and Kroemer, 2004; Thompson, 1995). Defects in apoptosis contribute to the development of numerous human diseases.

Apoptosis is not the only mechanism for programmed cell death. Recent studies have led to the identification of several other cell death processes that appear to be programmed but distinctive from apoptosis (Bergsbaken et al., 2009; Blum et al., 2012; Vanden Berghe et al., 2014; Yuan and Kroemer, 2010). The RIP3-dependent necrosis pathway is one of such processes (Moriwaki and Chan, 2013; Vandenabeele et al., 2010). RIP3-dependent necrosis can be triggered by tumor necrosis factor-α (TNFα) and is mediated by a signaling cascade involving protein kinases RIP1 (Degterev et al., 2008) and RIP3 (Cho et al., 2009; He et al., 2009; Kaiser et al., 2011; Newton et al., 2014; Oberst et al., 2011; Zhang et al., 2009), leading to activation of the downstream necrotic response. Up to date, the precise physiological function of RIP3-dependent necrosis has not been unambiguously established. However, mounting evidence suggests that it may benefit the organism under various infectious or inflammatory conditions (Cho et al., 2009; He et al., 2009; Murphy et al., 2013; Sun et al., 2012).

Recently, another form of regulated necrosis, known as ferroptosis, has been identified. It was shown that a synthetic compound, erastin, can induce a form of non-apoptotic cell death that requires iron (thus the name ferroptosis) (Dixon et al., 2012; Yagoda et al., 2007). Subsequent studies demonstrate that erastin inhibits cystine import and downstream glutathione synthesis, leading to deregulated cellular redox homeostasis and ultimately cell death (Dixon et al., 2012; Yang et al., 2014). Ferroptosis inhibition has been shown to be

effective in treating diseases such as ischemia/reperfusion-induced organ damage in experimental models (Friedmann Angeli et al., 2014; Linkermann et al., 2014). Further, because cancer cells harboring oncogenic Ras appear to be more sensitive to ferroptosis induction, this form of cell death has also being explored for cancer treatment (Yagoda et al., 2007; Yang et al., 2014). Although ferroptosis is strongly implicated in human diseases, currently the precise molecular mechanisms and biological functions of ferroptosis remain to be poorly understood.

This study reports the discovery of essential components and mechanisms for ferroptosis regulation, as well as an intimate functional interplay between ferroptosis and cellular metabolism. We identified transferrin and L-glutamine as extracellular regulators of ferroptosis. We also demonstrated that both transferrin transport and the cellular metabolic process glutaminolysis are essential for ferroptosis triggered by deprivation of full amino acids or of cystine alone. Further, we present evidence to support that glutaminolysis is a potential therapeutic target for treating heart injury caused by ischemia-reperfusion, likely due to the essential role of glutaminolysis in ferropotosis.

RESULTS

Serum Can Induce RIP3-Independent Necrosis upon Amino Acid Starvation

Nutrient availability is one of the key parameters for cells to make life-or-death decisions. It has been documented that long-term deprivation of growth factors, amino acids, or glucose causes gradual cell death (Wei et al., 2001). Although apoptotic machinery is often elicited in such starvation-induced death, this nevertheless can be considered a passive death process due to failure of the cell to survive the stressful conditions of nutrient/growth factor deprivation.

To recapitulate cell death under nutrient/growth factor deprivation, we incubated mouse embryonic fibroblasts (MEFs) in growth medium containing glucose but lacking amino acids and serum. Modest cell death was observed after 12 hrs (Figure 1A). We then incubated MEFs in amino acid-free medium containing full serum, expecting that growth factors in serum would mitigate cell death. Surprisingly, we observed much more potent cell death (Figure 1A), which was further confirmed by propidium iodide (PI) staining (Figure 1A, B) and measurement of cellular ATP levels (Figure 1C).

We subsequently investigated the molecular nature of this serum-induced cell death process. Cell death induced by combined deprivation of amino acids and serum was typical apoptosis, associated with caspase activation (Figure 1D) and characteristic morphological changes, such as chromosomal condensation, membrane blebbing, and formation of apoptotic bodies (Movie S1). However, in the presence of serum, although cell death was significantly more potent, there was no caspase activation (Figure 1D). Consistently, use of the pan-caspase inhibitor zVAD-FMK or deletion of *bax* and *bak*, genes essential for mitochondria-mediated apoptosis, failed to block such serum-induced cell death (Figure S1A, B). Further, the morphological changes associated with this cell death process were distinct from apoptosis (Figure 1E; Movies S2, S3). These results demonstrate that upon amino acid starvation, serum can induce non-apoptotic cell death in MEFs.

Through live cell time-lapse imaging, we observed that this cell death process shared key morphological features with necrosis, including cell rounding, swelling and plasma membrane rupture (Figure 1E; Movies S2, S3). Recent studies have established a programmed necrosis pathway dependent on the protein kinase RIP3 (Cho et al., 2009; He et al., 2009; Zhang et al., 2009). However, RIP3 gene deletion did not prevent serum-induced cell death in MEFs, although it completely blocked TNFα-induced necrosis as predicted (Figure 1F, G and Figure S1C). These results indicate that the RIP3-dependent necrosis pathway is not responsible for this serum-induced cell death.

Importantly, induction of potent cell death by serum under the condition of amino acid starvation can be observed in various types of cancerous and noncancerous cells. While amino acid/serum-double starvation could induce different levels of death in a time- and cell type-dependent manner, addition of serum unanimously further potentiated cell death in these cells (Figure S2).

Multiple Serum Factors Are Required for the Induction of Serum-Dependent Necrosis

Results in Figure 1 indicate that certain serum factor(s) is responsible for the activation of this type of RIP3-independent necrosis. Biologically active components in serum include both macromolecules (such as proteins) and small molecules. We removed small molecules in fetal bovine serum (FBS) by dialysis and then tested whether the dialyzed FBS (diFBS) can induce cell death upon amino acid starvation. Unlike full FBS, diFBS failed to induce potent cell death, and it even protected against the modest apoptotic cell death induced by amino acid/serum-double starvation in MEFs (Figure 2; Movie S4), presumably due to pro-survival growth factors presented in serum. The small molecule fraction of FBS (smFBS) prepared by filtering FBS through a size-exclusion membrane also failed to mimic the death-inducing activity of FBS. Only a combination of diFBS with smFBS fully restored the potent killing (Figure 2). Therefore, multiple serum factors, of both macromolecule and small molecule natures, are required to induce this form of necrosis upon amino acid starvation.

Transferrin Is Required for Serum-Dependent Necrosis

To identify the active component(s) in diFBS, we fractionated diFBS by ammonium sulfate precipitation in combination with various chromatographic columns. The killing activity of each fraction was monitored by incubating the fraction with cultured cells freshly switched to amino acid/serum-free medium, supplemented with the smFBS fraction. Cell death was measured after incubation for 12 hrs. In this assay, we used *bax/bak*-double knockout (DKO) MEFs to avoid amino acid/serum double starvation-induced apoptosis. After a four-step fractionation procedure (Figure 3A), we purified a single protein (Figure 3B) that correlated with killing activity (Figure 3C). Mass spectrometry analysis revealed the identity of the protein to be bovine transferrin. To validate this activity of transferrin, we immuno-depleted transferrin from FBS, and found that the death-inducing activity of FBS was indeed dramatically decreased (Figure 3D). Further, upon amino acid starvation, addition of commercial bovine holo-transferrin induced robust cell death in the presence of smFBS (Figure S3). The effective concentration of transferrin in these assays was well within the range of serum transferrin concentration (0.49–2.63 mg/ml) (Valaitis and Theil, 1984). To

rule out the possibility that the killing activity came from certain serum molecules co-purified with transferrin instead of transferrin per se, we tested recombinant human holo-transferrin that was expressed in rice (thus serum was not involved in the expression and purification). Again, upon amino acid starvation and in the presence of smFBS, recombinant human holo-transferrin could induce cell death in a dose-dependent manner (Figure 3E).

Transferrin is an iron carrier protein in serum that can be transported into the cell via receptor-mediated endocytosis (Andrews and Schmidt, 2007). To determine whether transferrin needs to be imported into the cell to exert its death-inducing function, we first tested the requirement of transferrin receptor (TfR) for serum-induced cell death. Indeed, TfR RNAi significantly inhibited cell death (Figure 3F). Transferrin can only interact with TfR and be transported into the cell when it is loaded with iron. Consistently, iron-free bovine apo-transferrin does not possess killing activity (Figure 3G), and multiple iron chelators can inhibit cell death (Figure 3H), in agreement with the requirement of transferrin import for this mode of cell death.

Glutamine and Glutaminolysis Are Required for Serum-Dependent Necrosis

To identify the small molecule component of FBS required for death induction, the smFBS fraction was subjected to multiple steps of fractionation (Figure 4A). The resulting fractions of each step were assessed for the death-inducing activity in MEFs in combination with diFBS. The active fractions obtained from the last step of purification (reverse phase-C18 HPLC) were analyzed by mass spectrometry. Three major mass peaks showed mass equal to that of two abundant components of serum: L-glutamine (146 Da, with Na^+ or H^+) and glucose (180 Da, with Na^+) (Figure 4B). Glucose failed to recapitulate the killing activity in combination with diFBS or transferrin, which was expected, because the cells were cultured in high-glucose medium and diFBS alone could not induce cell death upon amino acid starvation.

To determine whether glutamine (Gln) plays a role in serum-dependent necrosis, we compared L-Gln with several related amino acids. In a dose-dependent manner and upon amino acid starvation, L-Gln but not D-Gln or other tested amino acids induced potent cell death in the presence of diFBS (Figure 4C). To rule out the possibility that the killing activity is due to a degraded product rather than L-Gln itself, we tested a chemically stable L-Gln replacement, L-alanine-L-glutamine (A–Q). A–Q in combination with diFBS was also able to induce cell death upon amino acid starvation (Figure S4). Further, as expected, the requirement of diFBS in this assay can be replaced with transferrin (Figure 4D). In this later experiment, *bax/bak*-DKO MEFs were used to avoid apoptosis induced by amino acid/serum-double starvation. It should be noted that unlike in wild-type (WT) MEFs, L-Gln alone induced modest but measurable cell death in *bax/bak*-DKO MEFs, and addition of transferrin further enhanced cell death (Figure 4D).

L-Gln is the most abundant amino acid in the body. Through glutaminolysis, proliferating cells use L-Gln both as a nitrogen source for the biosynthesis of nucleotides, amino acids, and hexamine, and as an important carbon source for the tricarboxylic acid (TCA) cycle (DeBerardinis et al., 2008). We sought to identify the molecular basis underlying the role of L-Gln and glutaminolysis in serum-dependent necrosis. L-Gln uptake is mainly dependent

on receptors SLC38A1and SLC1A5 (McGivan and Bungard, 2007) (Figure 5A). We found that pharmacological inhibition of SLC1A5 by L-g-glutamyl-p-nitroanilide (GPNA) (Esslinger et al., 2005) or RNAi knockdown of these receptors markedly blocked serum-dependent necrosis (Figure 5B, C and Figure S5A), indicating that efficient import of L-Gln is essential for this type of cell death. In cells, Gln is converted into glutamate (Glu) by glutaminases (GLS) (Curthoys and Watford, 1995). Compound 968 (968), an inhibitor of GLS (Wang et al., 2010), significantly inhibited serum-dependent necrosis (Figure 5B). There are two isoforms of mammalian GLS, GLS1 and GLS2 (Curthoys and Watford, 1995). We found that knockdown of GLS2 but not GLS1 inhibited serum-dependent necrosis in MEFs (Figure 5D and Figure S5B). Consistently, Bis-2-(5-phenylacetamido-1,3,4-thiadiazol-2-yl)ethyl sulfide (BETPS), a GLS1-specific inhibitor (Robinson et al., 2007), failed to block serum-dependent necrosis in MEFs (Figure S5C). Whether the specific requirement of GLS2 but not GLS1 is due to differential regulation of these two enzymes or due to predominant expression of GLS2 in MEFs requires further investigation.

Downstream of glutaminolysis, glutamate can be further converted into α-ketoglutarate (α-KG) either by glutamate dehydrogenase (GLUD1)-mediated glutamate deamination or by transaminases-mediated transamination (Hensley et al., 2013) (Figure 5A). We found that amino-oxyacetate (AOA), a pan inhibitor of transaminases (Wise et al., 2008), could inhibit serum-dependent necrosis but not TNFα-induced apoptosis in MEFs (Figure 5B and Figure S5E). Consistently, RNAi of the transaminase GOT1 inhibited serum-dependent necrosis in MEFs (Figure 5E). However, GLUD1 RNAi failed to do so (Figure S5D).

We then explored whether downstream metabolites of glutaminolysis can mimic the killing activity of L-Gln. Indeed, upon amino acid starvation, α-KG in combination with diFBS can induce potent cell death even in the presence of transaminase inhibitor AOA (Figure 5F). This result is consistent with the fact that in the glutaminolysis pathway, α-KG is a downstream metabolite of transaminases, the target of AOA.

Serum-Dependent Necrosis Requires Cystine Starvation and Subsequent Depletion of Cellular Glutathione

Does serum-dependent necrosis require deprivation of all amino acids or certain specific amino acid(s)? To address this question, we examined which amino acid(s) can rescue cells from necrosis triggered by serum, or transferrin in combination with L-Gln, upon full amino acid starvation. Adding back a single amino acid, cysteine or cystine, but no other amino acids, rescued cells from death (Figure 6A, Figure S6A and S6B). Conversely, cystine starvation alone, in the presence of all other amino acids and serum, is sufficient to induce cell death (Figure 6B). Further, even a partial starvation of cystine can induce necrosis in a glutamine dose-dependent manner (Figure S6C).

As a building block of the cellular reducing agent glutathione, cysteine is required for maintaining cellular redox homeostasis. Therefore, it is likely that cysteine starvation induces cell death via depleting cellular glutathione (GSH) and consequently increasing reactive oxygen species (ROS). For this reason, we determined the cellular GSH and ROS levels under conditions that trigger serum-dependent necrosis. Indeed, these conditions

caused dramatic decrease of GSH level and increase of ROS level in cells (Figure 6C, D). Supplement of GSH or the biosynthetic precursor of GSH, N-acetylcysteine (NAC), or ROS scavenger Trolox (6-hydroxy-2,5,7,8-tetramethylchroman-2-carboxylic acid) all effectively blocked cell death under these conditions (Figure 6E, F). Further, RNAi knockdown of glutamate cysteine ligase catalytic subunit (GCLC), an essential enzyme for GSH synthesis, sensitized cell death induced by cystine starvation (Figure 6G). In addition, when mitochondrial oxidative phosphorylation, an important resource for ROS production, was inhibited by oligomycin, serum-induced necrosis was greatly reduced (Figure S6D).

Serum-Dependent Necrosis Is Ferroptosis

Requirement of cystine starvation, cellular glutathione depletion, and iron-carrier transferrin led us to test whether serum-dependent necrosis is the same as ferroptosis, a recently-discovered regulated necrosis process triggered by the synthetic chemical compound erastin and dependent on iron (Dixon et al., 2012; Dolma et al., 2003; Yagoda et al., 2007). Erastin triggers ferroptosis by inhibiting cystine uptake and thus depleting cellular glutathione (Dixon et al., 2012; Yang et al., 2014). The following experiments confirmed that serum-dependent necrosis is indeed ferroptosis, or at least these two modes of cell death share central mechanisms. First, ferrastatin-1 (Fer-1), a specific ferroptosis inhibitor (Dixon et al., 2012), can block serum-dependent cell death triggered by either full amino acid starvation or cystine starvation (Figure 7A). Second, both transferrin and glutamine were required for erastin-induced ferroptosis (Figure 7B). Further, iron chelators (DFO and CPX), glutaminolysis inhibitors Compound 968, and AOA can also inhibit erastin-induced ferroptosis (Figure 7C–D), demonstrating that ferroptosis requires the cellular metabolic process glutaminolysis.

Previous studies suggest that ferroptosis depends on Ras-ERK signaling and can be completely blocked by MEK inhibition (Yagoda et al., 2007). We found that this conclusion is inaccurate, likely due to the use of MEK inhibitor U0126 in the previous studies. We compared U0126 with a more selective and potent MEK1/2 inhibitor, PD0325901, and found that U0126 but not PD0325901 is able to block cell death induced by either erastin or amino acid starvation in the presence of serum (Figure S7A). Therefore, MEK activity is not essential for ferroptosis. The unintended effect of U0126 may be due to off-target inhibition of certain unknown enzymes required for ferroptosis, it might also be due to the anti-oxidative property of this compound as measured by its ability to reduce 2,2-Diphenyl-1-picrylhydrazyl (DPPH) (Figure S7B). It should also be noted that PD0325901 and Compound 968 showed no anti-oxidant function (Figure S7B).

Inhibitors of Glutaminolysis Prevent Heart Injury Induced by Ischemia-Reperfusion

Recent studies indicate that ferroptosis is associated with ischemia-reperfusion injury of organs such as liver and kidney, and is thus a potential therapeutic target (Friedmann Angeli et al., 2014; Linkermann et al., 2014). Since we identified glutaminolysis as an essential factor for ferroptosis, we sought to test if the glutaminolysis inhibitor Compound 968 might also be able to reduce ischemia-reperfusion injuries in an ex vivo heart model. We subjected the hearts isolated from wild-type mice to ischemia-reperfusion stress (Figure 7E). At the end of reperfusion, the hearts treated with either iron chelator DFO, a documented

ferroptosis inhibitor (Dixon et al., 2012), or GLS inhibitor Compound 968 showed significant improved function than hearts treated with vehicle (DMSO) as assessed by measuring the left ventricular developed pressure (LVDP) (Figure 7F; vehicle 43.20% ± 1.66% of Baseline, DFO 64.75% ± 4.09% and Compound-968 75.25% ± 5.75%). This functional improvement was consistent with the reduction in myocardial infarcts size (Figure 7G; vehicle treatment 30.82% ± 0.57% of myocardium, DFO treatment 22.60% ± 0.97%, and Compound-968 treatment 17.36% ± 0.47%). Similarly, DFO or compound-968 significantly inhibited the release of lactate dehydrogenase (LDH) during reperfusion, another indicator of myocardial injury (Figure 7H). These data suggest that inhibition of ferroptosis via ablating glutaminolysis can protect heart tissue from ischemia-reperfusion injury.

DISCUSSION

Collectively, our study uncovered several essential components and regulatory mechanisms for ferroptosis, a RIP3-independent programmed necrosis process. Extracellularly, serum components L-glutamine and transferrin were identified here as crucial regulators of ferroptosis. Intracellularly, the specific metabolic pathway glutaminolysis and components mediating transferrin import are required for ferroptosis. Several intriguing and seemingly counter-intuitive observations are associated with these findings: under normal conditions, both transferrin and glutamine are required for cell survival and growth. However, upon amino acid starvation, these growth/survival factors function to unleash ferroptotic cell death that is more rapid and potent than that caused by amino acid starvation alone. Such unexpected function of transferrin and glutamine is reminiscent of the pro-death function of the life-essential protein cytochrome c in the intrinsic apoptotic pathway. Similarly, glutaminolysis is crucial for cellular biosynthesis and proliferation, but here it is actively involved in and essential for this intriguing metabolic cell death process.

Under what biological conditions can ferroptosis, a necrotic process induced experimentally by cystine starvation or blockage of cystine uptake, occur? Because both transferrin and glutamine are highly abundant in blood whereas cystine amount is much lower, and a partial deprivation of cystine is sufficient to induce necrosis (Figure S6C), it is possible that under certain pathological conditions such as ischemia, cells might be susceptible to ferroptosis. Alternatively, blockage of cystine uptake or deficiency in glutathione synthesis can also lead to ferroptosis. Indeed, there are hemolytic anemia patients carrying hereditary deficiency of the glutathione synthetase (GSS) gene (Njalsson, 2005) or that of gamma-glutamyl cysteine synthetase (GCS) gene (Beutler et al., 1999; Dolma et al., 2003; Hirono et al., 1996; Manu Pereira et al., 2007; Ristoff et al., 2000). These patients might also be subject to higher risk of ferroptosis.

This study raised many important mechanistic questions for further understanding of ferroptosis. How do transferrin, cellular glutaminolysis, glutathione synthesis, and cellular ROS generation process communicate with each other to lead to cell death? Further, are the extracellular cues of ferroptosis regulated? There are a variety of potential mechanisms for such extracellular regulation. For example, we found that the killing activity of transferrin is dictated by its iron-loading status, thus mechanisms controlling iron-loading of transferrin

may impact ferroptosis. Additionally, blood glutamine concentration can be variable. Indeed, when we used different FBS preparations, we found that death-inducing activity ranged from very potent, modest, to almost undetectable (Figure S7C, D). Strikingly, we found a positive correlation between the killing activity of individual FBS preparations and their L-Gln concentrations, and addition of L-Gln or the smFBS fraction prepared from death-competent FBS can restore the killing activity of those inactive FBS preparations (Figure S7D–F).

Relevant to human disease, this study provided further evidence to support that ferroptosis is responsible, at least partially, for organ injury triggered by ischemia-reperfusion. This study also demonstrated that enzymes involved in glutaminolysis are potential therapeutic targets because of their crucial role in ferroptosis. Furthermore, the cancer therapeutic potential of ferroptosis should also be explored. Previous studies have linked ferroptosis with oncogenic Ras, and most recently, it has been demonstrated that p53 tumor suppressor positively regulates ferroptosis by transcriptionally inhibiting the expression of the cystine/glutamate antiporter SLC7A11 (Dixon et al., 2012; Jiang et al., 2015; Yagoda et al., 2007). In light of our finding that ferroptosis requires glutaminolysis, a metabolic pathway highly active in cancer tissues and essential for cancer growth, can ferroptosis be preferentially triggered in cancer cells as a therapeutic option?

EXPERIMENTAL PROCEDURES

For full experimental procedures, see the Supplemental Information.

Induction and measurement of cell death

To induce cell death, 80%-confluent cells were washed with PBS twice, and then cultured in amino acid-free medium, with specific factors added as indicated in individual experiments. Cell death was analyzed by propidium iodide (PI) staining coupled with microscopy or flow cytometry. Alternatively, cell viability was determined using the CellTiter-Glo luminescent Cell Viability Assay (Promega). In assays using WT MEFs, viability was calculated by normalizing ATP levels to cells treated with amino acid-starvation in the presence of 10% (v/v) diFBS, while in assays using *bax/bak*-DKO MEFs, ATP levels were normalized to cells treated with amino acid and FBS double starvation.

Purification and identification of transferrin from FBS

All purification steps were carried out at 4°C, and chromatography was performed with an Amersham FPLC system. For the purification, 20 ml FBS (664 mg protein) was applied to 50–70 % (saturation) ammonium sulfate precipitation. The protein pellet (242 mg) that contained the activity was dissolved in 4 ml Buffer A (20 mM Hepes, PH 7.5 10 mM NaCl) and dialyzed overnight. The activity was applied to HiTrap SP Sepharose (GE Healthcare). The flow-through containing the activity was subjected to HiTrap Q Sepharose (GE Healthcare). After washing the column with Buffer A, the fractions was eluted by a gradient of 10–300 mM NaCl in Buffer A. Activity-containing fractions were further fractionated with HiTrap Heparin Sepharose (GE Healthcare) by using a gradient 10–300 mM NaCl in Buffer A. Fractions of 1 ml was collected. After dialysis, filtered with 0.2 mM filter, the

fractions was assayed for activity. SDS-PAGE and Coomassie staining (Bio-Rad) was preformed, and a single band correlated with the killing activity was subject to protein identity determination by mass spectrometry analysis (MALDI-TOF-MS/MS). The activity was identified as bovine transferrin.

Immuno-depletion of transferrin

To deplete transferrin from serum, amino acid- free DMEM medium containing 10% FBS was incubated with control IgG or anti-bovine transferrin antibody bound to Protein G Agarose (GE Healthcare) overnight at 4°C. Protein G Agarose was removed by centrifugation and the supernatant was assayed for killing activity.

Purification and identification of L-glutamine from FBS

FBS was filtered through Centrifugal Filter Units (MWCO 10 KDa) (Millipore) to obtain small molecule fraction (smFBS). One ml of smFBS was dried under vacuum and dissolved in 1 ml methanol and insoluble material was removed by centrifugation. The supernatant was dried and dissolved in 750-μl methanol first and then mixed with 614-μl acetonitrile (final ratio of methanol: acetonitrile is 55:45). After incubating the mix for 30 min at 4°C, precipitated material was removed by centrifugation, and the supernatant was dried and dissolved in 750-μl methanol. Aliquot of 150-μl was mixed with 1350-μl acetonitrile (final ratio of methanol: acetonitrile is 10:90) and incubated for 30 min at 4°C. The insoluble material was obtained by centrifugation and then dissolved in 75-μl ddH_2O. An aliquot of 50-μl as input was applied to a reversed phase XDB-C18 (4.6 × 250 mm) HPLC analytical column (Agilent). Separation was achieved by use of step elution consisting of A (ddH_2O) and B (methanol) as following: 0.00–11.00 min: 100% A, flow rate 1 ml/min; 11.00–21.00 min: 100% B, flow rate 1 ml/min. All fractions were dried and dissolved in 100-μl ddH_2O, and 25-μl of each fraction was subjected to activity assay. The fraction with the highest killing activity was subjected to mass spectrometry (PE SCIEX API-100 LC/MS system, mass range: 30.0 to 500.0 by amu).

Time-lapse microscopy

Live cell imaging of H2b-mcherry expressing MEFs was performed on glass-bottom 6-well plates (MatTek, Ashland, MA) using a Nikon Ti-E inverted microscope attached to a CoolSNAP CCD camera (Photometrics). Fluorescence and differential interference contrast (DIC) images were acquired every 7 minutes, and images were analyzed using NIS elements software (Nikon) and ImageJ software (NIH). For confocal imaging, MEFs were grown on 35mm glass bottom plates (MatTek, Ashland, MA) and DIC images were acquired every 5 minutes with the Ultraview Vox spinning disc confocal system (Perkin Elmer) equipped with a Yokogawa CSU-X1 spinning disc head, and EMCCD camera (Hamamatsu C9100-13), and coupled with a Nikon Ti-E microscope. Image analysis was performed with Volocity software (Perkin Elemer). All imaging was carried out in incubation chambers at 5% CO_2 and 37°C.

GSH measurement

2×10^5 MEFs were seeded in 6-well plates. One day later, cells were treated as indicated for 6 hours. Cells were harvested and cell numbers were determined. Total glutathione was measured as described previously (Rahman et al., 2006).

Measurement of reactive oxygen species (ROS)

MEFs were treated as indicated, and then 10 μM 2′,7′-dichlorodihydrofluorescein diacetate (H_2DCFDA, Life Technologies Cat# D-399) was added and incubated for 1 hour. Excess H_2DCFDA was removed by washing the cells twice with PBS. Labeled cells were trypsinized and resuspended in PBS plus 5% FBS. Oxidation of H_2DCFDA to the highly fluorescent 2′,7′-dichlorofluorescein (DCF) is proportional to ROS generation and was analyzed using a flow cytometer (Fortessa, BD Biosciences). A minimum of 10,000 cells was analyzed per condition.

2,2-Diphenyl-1-picrylhydrazyl Assay for antioxidant activity

The experiment was performed as described previously (Blois, 1958; Dixon et al., 2012). 2,2-Diphenyl-1-picrylhydrazyl (DPPH) (Sigma Cat#D9132) was dissolved in methanol to a final concentration of 50 μM. The tested compounds were added to 1 ml of DPPH solution with a final concentration of 50 μM. Samples were mixed well and incubated at room temperature for 1 hr. The absorbance at 517 nm (indicating the concentration of non-reduced DPPH) was measured using methanol as control. Results were normalized to DMSO (which has no antioxidant activity; set as 100%).

Ischemia-reperfusion (I/R) analysis using isolated hearts

Male C57BL/6J mice weighing 25–30 g at age 12–14 weeks were used in all experiments and maintained in a temperature-controlled room with alternating 12:12-h light-dark cycles. Experiments were performed using an isovolumic isolated heart preparation as published and modified for the use in mice hearts (Ananthakrishnan et al., 2009; Hwang et al., 2004). Hearts from 12–14 weeks aged wild-type mice were isolated, and retrograde perfused at 37°C in a non-recirculating mode through the aorta at a rate of 2.5 ml/min. Hearts were perfused with modified Krebs-Henseleit (KH) buffer (118 mM NaCl, 4.7 mM KCl, 2.5 mM $CaCl_2$, 1.2 mM $MgCl_2$, 25 mM $NaHCO_3$, 5 mM glucose, 0.4 mM palmitate, 0.2 mM glutamine, 10 μg/ml human recombinant transferrin, 0.4 mM BSA, and 70 mU/l insulin). Left ventricular developed pressure (LVDP) was measured using a latex balloon in the left ventricle. LVDP and coronary perfusion pressure were monitored continuously on a four-channel Gould recorder. Hearts were perfused either with KH buffer containing vehicle (DMSO) or the Compounds throughout the I/R protocol. After an equilibration period of 30 min, global ischemia was performed for 30 min followed by 60 minutes of reperfusion. Cardiac injury due to I/R stress was assessed by measuring LDH release in the perfusates that were collected during 60 min of reperfusion. Infarct area was measured using 2, 3, 5-triphenyltetrazolium chloride (TTC) staining. After 60 min of reperfusion, the heart is perfused with Evans blue in-situ and then removed. Hearts were sliced into cross-sections at approximately 1-mm intervals. The sections were embedded in the TTC solution at 37°C for 10 min, and area of infarct as a percent of the whole heart was quantified as described.

Functional recovery of LVDP was expressed by comparing to the initial LVDP before ischemia. All animal experiments were approved by the Institutional Animal Care and Use Committees of New York University School of Medicine and conformed to the guidelines outlined in the National Institutes of Health Guide for Care and Use of Laboratory Animals (NIH Pub. No. 85–23, 1996).

Statistical analyses

All statistical analyses were performed using Prism 5.0c GraphPad Software. P values were calculated with unpaired Student's t test. Data are presented as mean ± SEM from 3 independent experiments (*P < 0.05, **P < 0.01 ***P < 0.001 by unpaired Student t-test).

Supplementary Material

Refer to Web version on PubMed Central for supplementary material.

Acknowledgments

We thank Memorial Sloan Kettering Cancer Center (MSKCC) colleagues Drs. Ron Hendrickson and Hediye Erdjument-Bromage for identification of bovine transferrin by mass spectrometry, Drs. George Sukenick and Hui Fang for analyzing small molecule activity by mass spectrometry, and Dr. Michael Overholtzer and his lab members for assistance with live cell imaging. We also thank Drs. Junru Wang (MSKCC) and Qing Li (New York University) for technical support. This work is supported by NIH grants R01CA166413 (to XJ), R01GM113013 (to XJ), R01HL102022 (to RR), P01HL60901 (to RR), P01AG026467 (to RR), and Mr. William H. and Mrs. Alice Goodwin and the Commonwealth Foundation for Cancer Research of the Experimental Therapeutics Center of MSKCC (to XJ).

References

Ananthakrishnan R, Kaneko M, Hwang YC, Quadri N, Gomez T, Li Q, Caspersen C, Ramasamy R. Aldose reductase mediates myocardial ischemia-reperfusion injury in part by opening mitochondrial permeability transition pore. American journal of physiology Heart and circulatory physiology. 2009; 296:H333–341. [PubMed: 19060123]

Andrews NC, Schmidt PJ. Iron homeostasis. Annual review of physiology. 2007; 69:69–85.

Bergsbaken T, Fink SL, Cookson BT. Pyroptosis: host cell death and inflammation. Nat Rev Microbiol. 2009; 7:99–109. [PubMed: 19148178]

Beutler E, Gelbart T, Kondo T, Matsunaga AT. The molecular basis of a case of gammaglutamylcysteine synthetase deficiency. Blood. 1999; 94:2890–2894. [PubMed: 10515893]

Blois MS. Antioxidant Determinations by the Use of a Stable Free Radical. Nature. 1958; 181:1199–1200.

Blum ES, Abraham MC, Yoshimura S, Lu Y, Shaham S. Control of Nonapoptotic Developmental Cell Death in Caenorhabditis elegans by a Polyglutamine-Repeat Protein. Science. 2012; 335:970–973. [PubMed: 22363008]

Budihardjo I, Oliver H, Lutter M, Luo X, Wang X. Biochemical pathways of caspase activation during apoptosis. Annual review of cell and developmental biology. 1999; 15:269–290.

Cho YS, Challa S, Moquin D, Genga R, Ray TD, Guildford M, Chan FK. Phosphorylation-driven assembly of the RIP1-RIP3 complex regulates programmed necrosis and virus-induced inflammation. Cell. 2009; 137:1112–1123. [PubMed: 19524513]

Curthoys NP, Watford M. Regulation of glutaminase activity and glutamine metabolism. Annual review of nutrition. 1995; 15:133–159.

Danial NN, Korsmeyer SJ. Cell death: Critical control points. Cell. 2004; 116:205–219. [PubMed: 14744432]

DeBerardinis RJ, Lum JJ, Hatzivassiliou G, Thompson CB. The biology of cancer: metabolic reprogramming fuels cell growth and proliferation. Cell metabolism. 2008; 7:11–20. [PubMed: 18177721]

Degterev A, Hitomi J, Germscheid M, Ch'en IL, Korkina O, Teng X, Abbott D, Cuny GD, Yuan C, Wagner G, et al. Identification of RIP1 kinase as a specific cellular target of necrostatins. Nature chemical biology. 2008; 4:313–321. [PubMed: 18408713]

Dixon SJ, Lemberg KM, Lamprecht MR, Skouta R, Zaitsev EM, Gleason CE, Patel DN, Bauer AJ, Cantley AM, Yang WS, et al. Ferroptosis: an iron-dependent form of nonapoptotic cell death. Cell. 2012; 149:1060–1072. [PubMed: 22632970]

Dolma S, Lessnick SL, Hahn WC, Stockwell BR. Identification of genotype-selective antitumor agents using synthetic lethal chemical screening in engineered human tumor cells. Cancer cell. 2003; 3:285–296. [PubMed: 12676586]

Esslinger CS, Cybulski KA, Rhoderick JF. Ngamma-aryl glutamine analogues as probes of the ASCT2 neutral amino acid transporter binding site. Bioorganic & medicinal chemistry. 2005; 13:1111–1118. [PubMed: 15670919]

Friedmann Angeli JP, Schneider M, Proneth B, Tyurina YY, Tyurin VA, Hammond VJ, Herbach N, Aichler M, Walch A, Eggenhofer E, et al. Inactivation of the ferroptosis regulator Gpx4 triggers acute renal failure in mice. Nature cell biology. 2014; 16:1180–1191. [PubMed: 25402683]

Fuchs Y, Steller H. Programmed Cell Death in Animal Development and Disease. Cell. 2011; 147:742–758. [PubMed: 22078876]

Green DR, Kroemer G. The pathophysiology of mitochondrial cell death. Science. 2004; 305:626–29. [PubMed: 15286356]

He S, Wang L, Miao L, Wang T, Du F, Zhao L, Wang X. Receptor interacting protein kinase-3 determines cellular necrotic response to TNF-alpha. Cell. 2009; 137:1100–1111. [PubMed: 19524512]

Hensley CT, Wasti AT, DeBerardinis RJ. Glutamine and cancer: cell biology, physiology, and clinical opportunities. The Journal of clinical investigation. 2013; 123:3678–3684. [PubMed: 23999442]

Hirono A, Iyori H, Sekine I, Ueyama J, Chiba H, Kanno H, Fujii H, Miwa S. Three cases of hereditary nonspherocytic hemolytic anemia associated with red blood cell glutathione deficiency. Blood. 1996; 87:2071–2074. [PubMed: 8634459]

Hwang YC, Kaneko M, Bakr S, Liao H, Lu Y, Lewis ER, Yan S, Ii S, Itakura M, Rui L, et al. Central role for aldose reductase pathway in myocardial ischemic injury. FASEB journal: official publication of the Federation of American Societies for Experimental Biology. 2004; 18:1192–1199. [PubMed: 15284219]

Jiang L, Kon N, Li TY, Wang SJ, Su T, Hibshoosh H, Baer R, Gu W. Ferroptosis as a p53-mediated activity during tumour suppression. Nature. 2015; 520:57. [PubMed: 25799988]

Kaiser WJ, Upton JW, Long AB, Livingston-Rosanoff D, Daley-Bauer LP, Hakem R, Caspary T, Mocarski ES. RIP3 mediates the embryonic lethality of caspase-8-deficient mice. Nature. 2011; 471:368–372. [PubMed: 21368762]

Linkermann A, Skouta R, Himmerkus N, Mulay SR, Dewitz C, De Zen F, Prokai A, Zuchtriegel G, Krombach F, Welz PS, et al. Synchronized renal tubular cell death involves ferroptosis. Proceedings of the National Academy of Sciences of the United States of America. 2014; 111:16836–16841. [PubMed: 25385600]

Manu Pereira M, Gelbart T, Ristoff E, Crain KC, Bergua JM, Lopez Lafuente A, Kalko SG, Garcia Mateos E, Beutler E, Vives Corrons JL. Chronic non-spherocytic hemolytic anemia associated with severe neurological disease due to gamma-glutamylcysteine synthetase deficiency in a patient of Moroccan origin. Haematologica. 2007; 92:e102–105. [PubMed: 18024385]

McGivan JD, Bungard CI. The transport of glutamine into mammalian cells. Frontiers in bioscience: a journal and virtual library. 2007; 12:874–882. [PubMed: 17127344]

Moriwaki K, Chan FK. RIP3: a molecular switch for necrosis and inflammation. Genes & development. 2013; 27:1640–1649. [PubMed: 23913919]

Murphy JM, Czabotar PE, Hildebrand JM, Lucet IS, Zhang JG, Alvarez-Diaz S, Lewis R, Lalaoui N, Metcalf D, Webb AI, et al. The pseudokinase MLKL mediates necroptosis via a molecular switch mechanism. Immunity. 2013; 39:443–453. [PubMed: 24012422]

Newton K, Dugger DL, Wickliffe KE, Kapoor N, de Almagro MC, Vucic D, Komuves L, Ferrando RE, French DM, Webster J, et al. Activity of protein kinase RIPK3 determines whether cells die by necroptosis or apoptosis. Science. 2014; 343:1357–1360. [PubMed: 24557836]

Njalsson R. Glutathione synthetase deficiency. Cell Mol Life Sci. 2005; 62:1938–1945. [PubMed: 15990954]

Oberst A, Dillon CP, Weinlich R, McCormick LL, Fitzgerald P, Pop C, Hakem R, Salvesen GS, Green DR. Catalytic activity of the caspase-8-FLIP(L) complex inhibits RIPK3-dependent necrosis. Nature. 2011; 471:363–367. [PubMed: 21368763]

Rahman I, Kode A, Biswas SK. Assay for quantitative determination of glutathione and glutathione disulfide levels using enzymatic recycling method. Nature protocols. 2006; 1:3159–3165. [PubMed: 17406579]

Ristoff E, Augustson C, Geissler J, de Rijk T, Carlsson K, Luo JL, Andersson K, Weening RS, van Zwieten R, Larsson A, et al. A missense mutation in the heavy subunit of gamma-glutamylcysteine synthetase gene causes hemolytic anemia. Blood. 2000; 95:2193–2196. [PubMed: 10733484]

Robinson MM, McBryant SJ, Tsukamoto T, Rojas C, Ferraris DV, Hamilton SK, Hansen JC, Curthoys NP. Novel mechanism of inhibition of rat kidney-type glutaminase by bis-2-(5-phenylacetamido-1,2,4-thiadiazol-2-yl)ethyl sulfide (BPTES). The Biochemical journal. 2007; 406:407–414. [PubMed: 17581113]

Sun L, Wang H, Wang Z, He S, Chen S, Liao D, Wang L, Yan J, Liu W, Lei X, et al. Mixed lineage kinase domain-like protein mediates necrosis signaling downstream of RIP3 kinase. Cell. 2012; 148:213–227. [PubMed: 22265413]

Thompson CB. Apoptosis in the Pathogenesis and Treatment of Disease. Science. 1995; 267:1456–1462. [PubMed: 7878464]

Valaitis AP, Theil EC. Developmental-Changes in Plasma Transferrin Concentrations Related to Red-Cell Ferritin. Journal of Biological Chemistry. 1984; 259:779–784. [PubMed: 6607254]

Vanden Berghe T, Linkermann A, Jouan-Lanhouet S, Walczak H, Vandenabeele P. Regulated necrosis: the expanding network of non-apoptotic cell death pathways. Nature reviews Molecular cell biology. 2014; 15:135–147. [PubMed: 24452471]

Vandenabeele P, Declercq W, Van Herreweghe F, Vanden Berghe T. The Role of the Kinases RIP1 and RIP3 in TNF-Induced Necrosis. Sci Signal. 2010; 3

Wang JB, Erickson JW, Fuji R, Ramachandran S, Gao P, Dinavahi R, Wilson KF, Ambrosio AL, Dias SM, Dang CV, et al. Targeting mitochondrial glutaminase activity inhibits oncogenic transformation. Cancer cell. 2010; 18:207–219. [PubMed: 20832749]

Wei MC, Zong WX, Cheng EH, Lindsten T, Panoutsakopoulou V, Ross AJ, Roth KA, MacGregor GR, Thompson CB, Korsmeyer SJ. Proapoptotic BAX and BAK: a requisite gateway to mitochondrial dysfunction and death. Science. 2001; 292:727–730. [PubMed: 11326099]

Wise DR, DeBerardinis RJ, Mancuso A, Sayed N, Zhang XY, Pfeiffer HK, Nissim I, Daikhin E, Yudkoff M, McMahon SB, et al. Myc regulates a transcriptional program that stimulates mitochondrial glutaminolysis and leads to glutamine addiction. Proceedings of the National Academy of Sciences of the United States of America. 2008; 105:18782–18787. [PubMed: 19033189]

Yagoda N, von Rechenberg M, Zaganjor E, Bauer AJ, Yang WS, Fridman DJ, Wolpaw AJ, Smukste I, Peltier JM, Boniface JJ, et al. RAS-RAF-MEK-dependent oxidative cell death involving voltage-dependent anion channels. Nature. 2007; 447:864–868. [PubMed: 17568748]

Yang WS, SriRamaratnam R, Welsch ME, Shimada K, Skouta R, Viswanathan VS, Cheah JH, Clemons PA, Shamji AF, Clish CB, et al. Regulation of ferroptotic cancer cell death by GPX4. Cell. 2014; 156:317–331. [PubMed: 24439385]

Yuan J, Kroemer G. Alternative cell death mechanisms in development and beyond. Genes & development. 2010; 24:2592–2602. [PubMed: 21123646]

Zhang DW, Shao J, Lin J, Zhang N, Lu BJ, Lin SC, Dong MQ, Han J. RIP3, an energy metabolism regulator that switches TNF-induced cell death from apoptosis to necrosis. Science. 2009; 325:332–336. [PubMed: 19498109]

Highlights

- Transferrin and glutamine are essential for the induction of ferroptotic cell death
- Transferrin import is required for ferroptosis
- The cellular metabolic process gltaminolysis is essential for ferroptosis
- Inhibiting glutaminolysis reduces ischemia/reperfusion-induced heart injury ex vivo

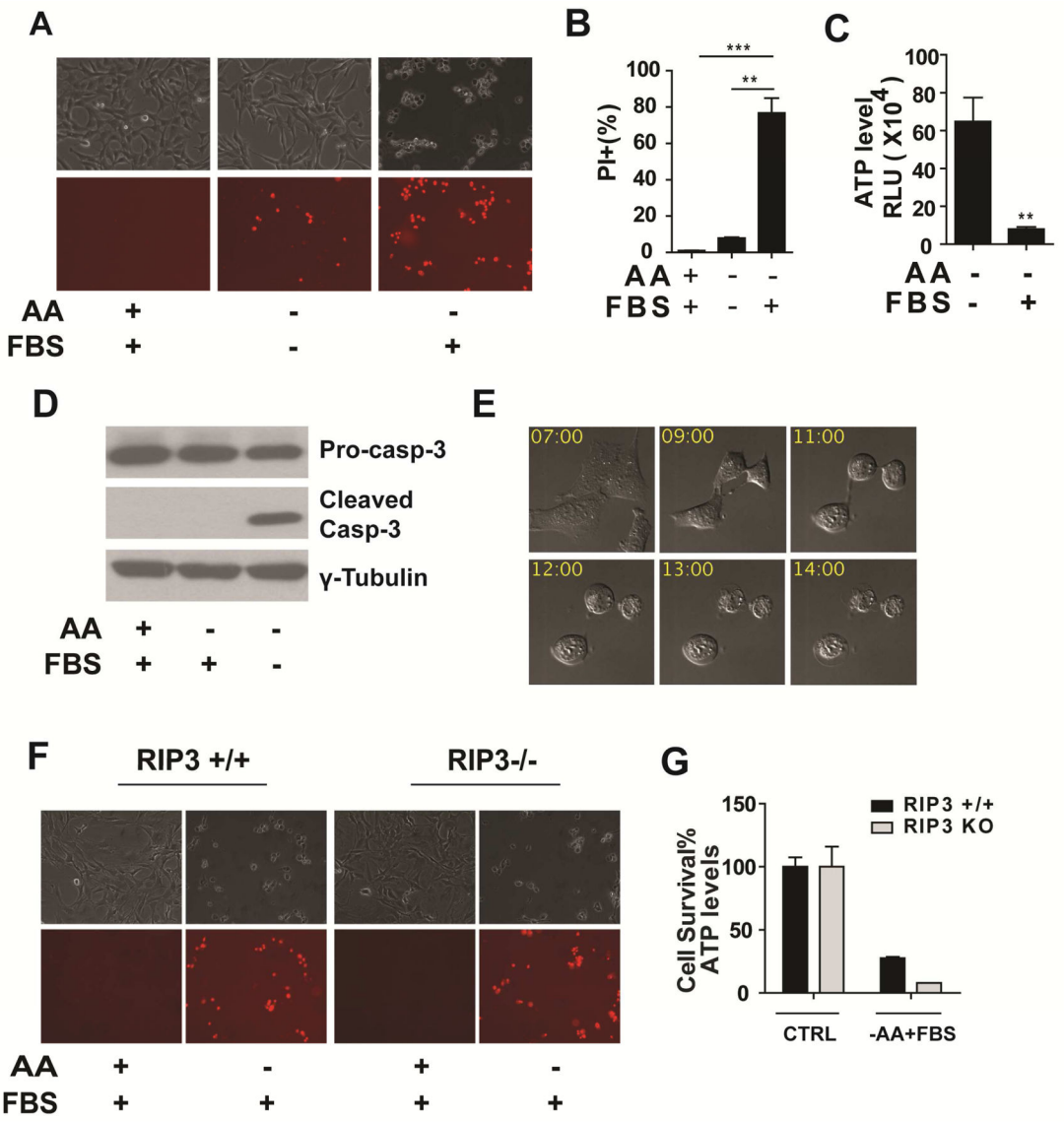

Figure 1. Serum induces potent non-apoptotic, RIP3-indepednent cell death upon amino acid starvation

(**A**) Microscopy showing cell death induced by serum upon amino acid starvation. MEFs were treated as indicated for 12 hrs. Upper panel: phase-contrast, lower panel: propidium iodide (PI) staining. AA: amino acids, FBS: 10% (v/v) Fetal Bovine Serum.

(**B**) Quantitation of cell death by PI-staining coupled with flow cytometry. Cells were subjected to the same treatment as in panel A. Quantitative data here and thereafter are presented as mean ± SEM from 3 independent experiments (*P < 0.05, **P < 0.01, ***P < 0.001 by unpaired Student t-test).

(**C**) Determination of cell viability by measuring cellular ATP levels. Cells were subjected to the same treatment as in panel A.

(**D**) Serum-induced cell death is independent of caspase activation. MEFs were treated as indicated for 12 hrs and caspase-3 activation was assessed by immunoblotting.

(**E**) Serum-induced cell death shows necrotic morphology. Representative still images from confocal time-lapse imaging of MEFs treated with amino acid starvation in the presence of FBS. Time (hr) after treatment is indicated.

(**F–G**) Serum-induced cell death is independent of RIP3. RIP3+/+ MEFs and RIP3−/− MEFs were treated as indicated. Cell death was monitored by phase-contract microscopy and PI-staining (F), and cell viability was determined by measuring cellular ATP levels (G). CTRL: control.

See also Figure S1 and Movies S1, S2 and S3

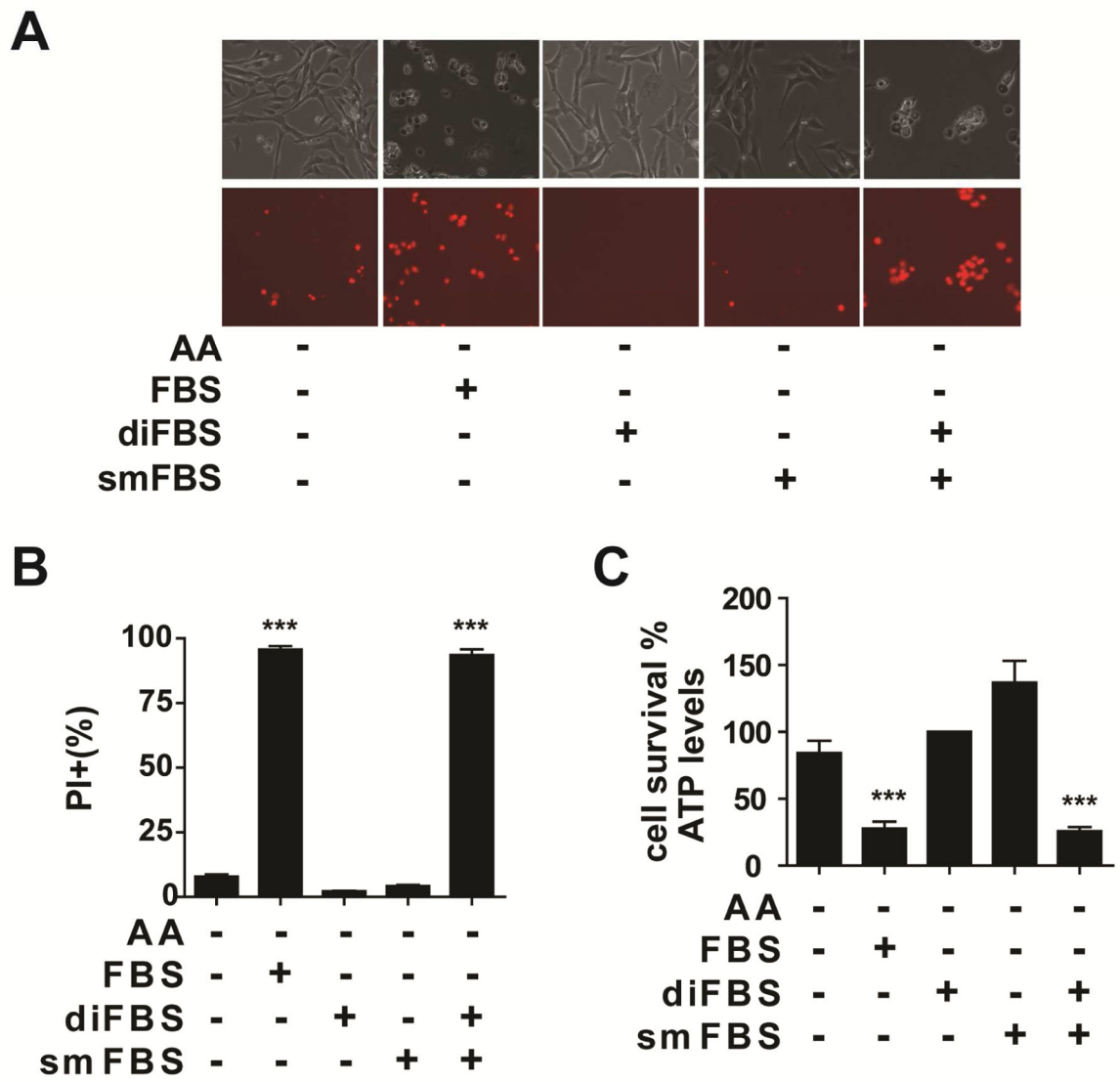

Figure 2. Multiple serum components are required for serum-induced cell death

(**A**) MEFs were treated as indicated for 12 hrs. Upper panel: phase-contrast, Lower panel: PI staining. diFBS: 10% (v/v) dialyzed FBS, smFBS: 10% (v/v).

(**B–C**) MEFs were treated as indicated for 12 hrs. Cell death was determined by PI staining coupled with flow Cytometry (B), and cell viability was determined by measuring cellular ATP levels (C).

See also Figure S2 and Movie S4

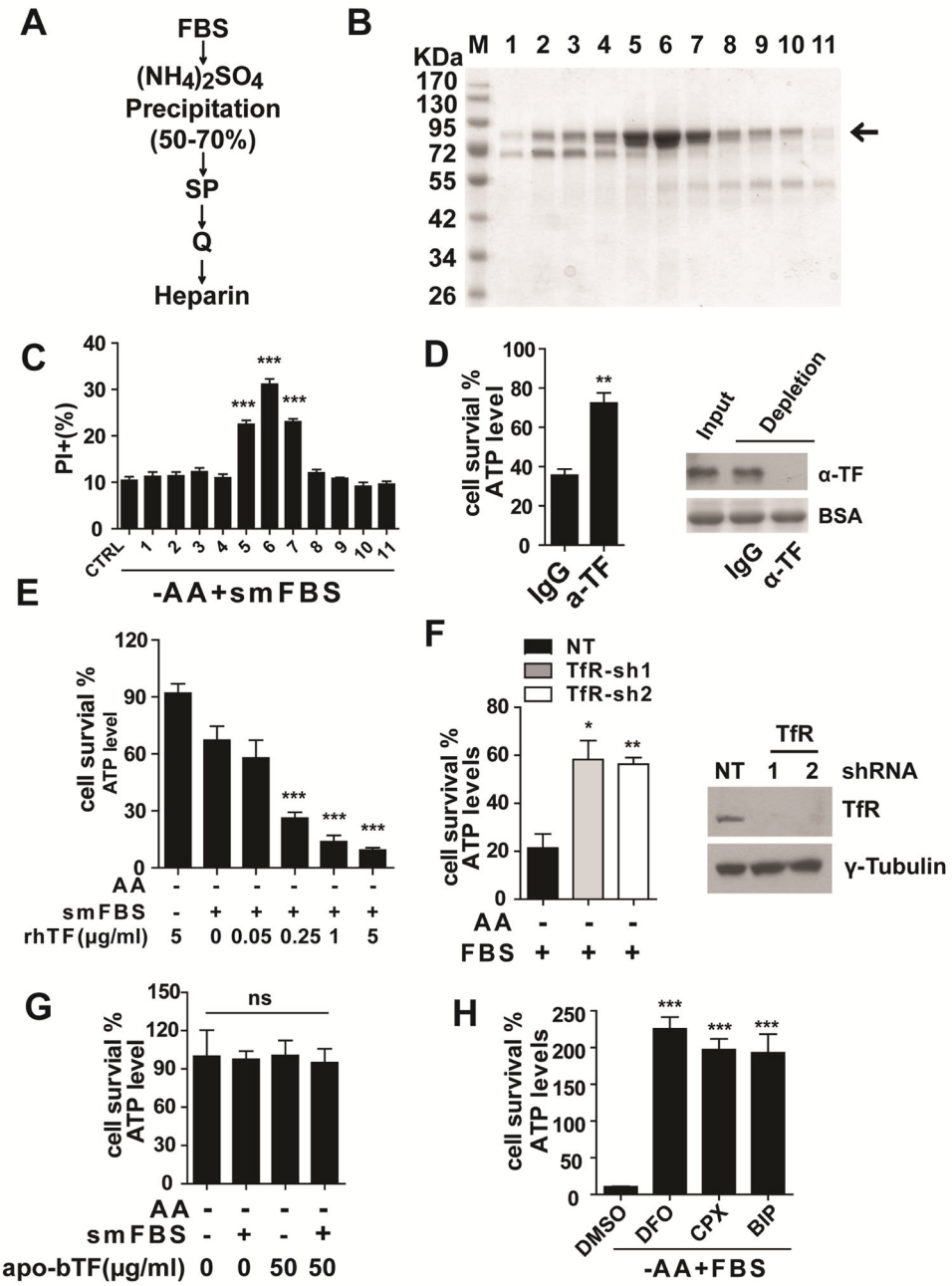

Figure 3. Transferrin and transferrin receptor are required for serum-dependent necrosis

(**A**) Purification scheme for the death-inducing component in diFBS. See Methods for detailed description.

(**B**) The final heparin column fractions were resolved by SDS-PAGE and stained with Coomassie blue. Arrow indicates the protein band correlating with killing activity.

(**C**) In amino acid-free medium, *bax/bak*-DKO MEFs were incubated with the heparin fractions in combination with smFBS as indicated, and cell death was determined by PI staining coupled with flow cytometry.

(**D**) Immuno-depletion of transferrin (TF) abrogated the killing activity of serum. Serum was immuno-depleted with control IgG or anti-transferrin antibody (α-TF) as indicated, and

subsequently used to induce cell death in *Bax/bak*-DKO MEFs under amino acid-free conditions for 12 hrs. Western blot showed the efficiency of transferrin depletion from FBS, with BSA as the loading control.

(**E**) Recombinant human holo-transferrin (rhTF) induced cell death in *Bax/bak*-DKO MEFs under amino acid-free conditions in a smFBS-dependent manner.

(**F**) RNAi of transferrin receptor (TfR) inhibited serum-dependent necrosis. MEFs expressing control shRNA (NT) or two independent shRNAs targeting TfR were treated as indicated for 12 hrs and cell viability was measured. Western blot (lower panel) confirmed knockdown of TfR expression.

(**G**) Iron-free bovine apo-transferrin (apo-bTF) did not have death-inducing activity.

(**H**) Iron chelators blocked serum-dependent necrosis. MEFs were treated with 3 different iron chelators as indicated, and cell viability was determined by measuring cellular ATP levels. DFO (Deferoxamine), 80 μM; CPX (ciclopirox olamine), 10 μM; BIP (2, 2-bipyridyl), 100 μM.

See also Figure S3

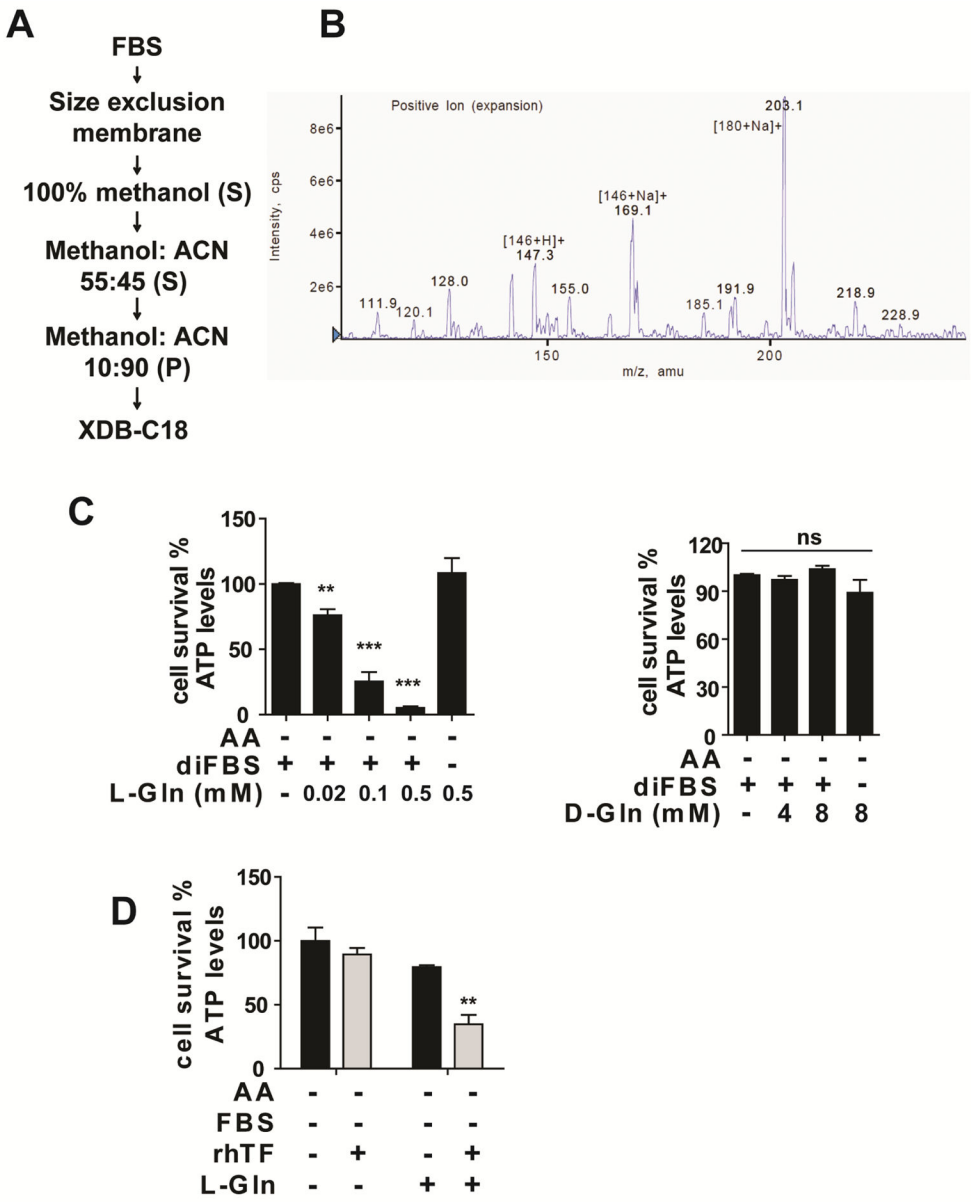

Figure 4. Glutamine is the death-inducing small molecule component in serum

(**A**) Purification scheme for the death-inducing small molecule component in FBS. S: supernatant; P: pellet. See Methods for detailed description.

(**B**) LC/MS spectra of the active fraction from the XDB-C18 column.

(**C**) L-Gln (left panel) but not D-Gln (right panel) induces cell death in a diFBS-dependent manner under AA starvation. MEFs were treated as indicated for 12 hrs and cell viability was subsequently measured.

(**D**) L-Gln in combination with transferrin recapitulated the cell death-inducing activity of serum. *bax/bak*-DKO MEFs were treated as indicated for 12 hrs and cell viability was subsequently measured. L-Gln concentration, 0.1 mM.

See also Figure S4

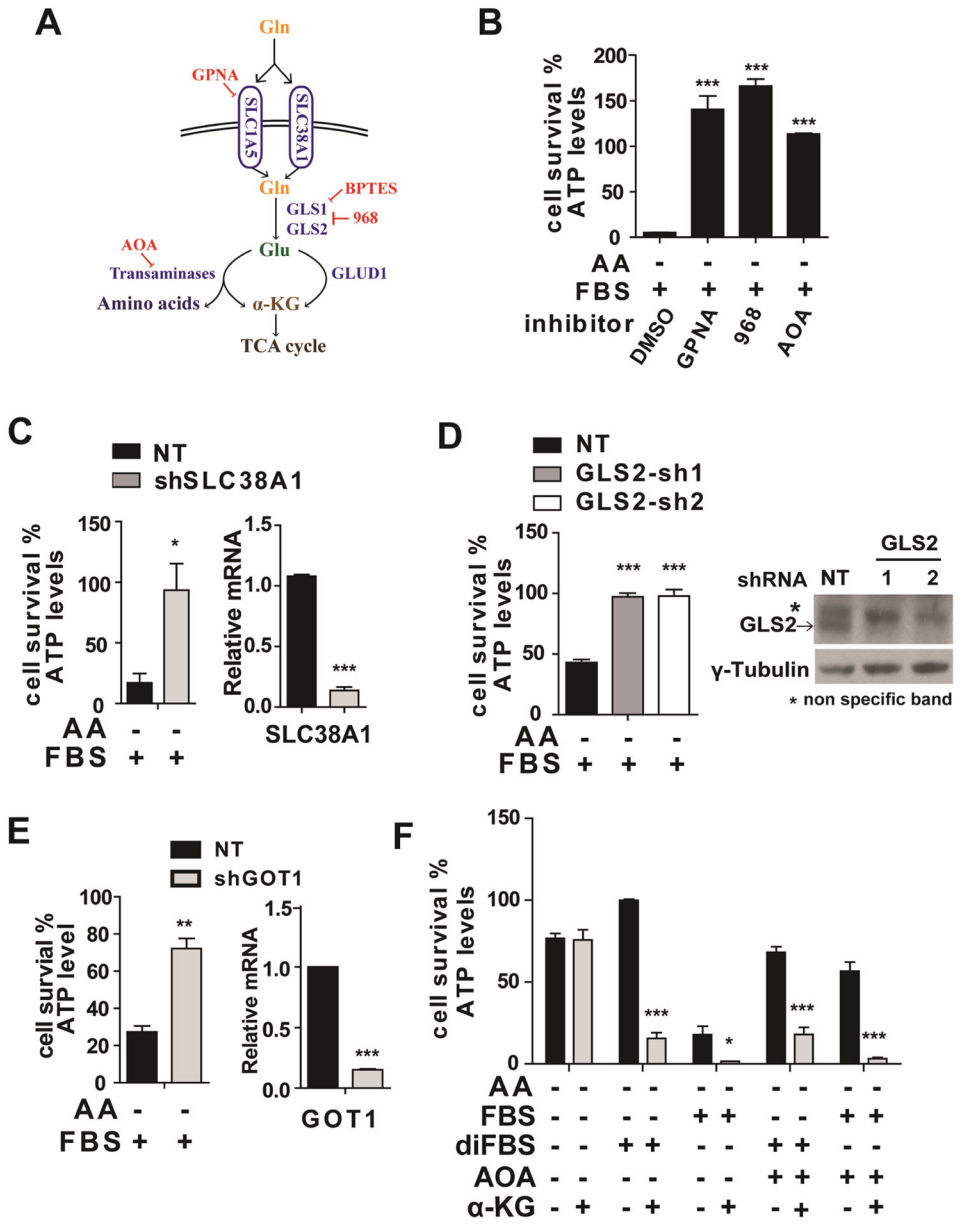

Figure 5. Glutaminolysis mediates serum-dependent necrosis

(**A**) Schematic overview of the glutaminolysis pathway.

(**B**) Pharmacological inhibition of multiple components in the glutaminolysis pathway abrogated serum-dependent necrosis. The following inhibitors were used as indicated: L-Gln transporter inhibitor GPNA (5 mM); GLS inhibitor compound 968 (968, 20 μM); Pan-transaminases inhibitor AOA (0.5 mM).

(**C**) RNAi knockdown of SLC38A1 inhibited serum-dependent necrosis. Left: MEFs expressing non-targeting (NT) shRNA or shRNA targeting SLC38A1 were treated as indicated for 12 hrs and cell viability was subsequently measured. Right: qPCR measurement of SLC38A1 mRNA levels in MEFs infected with NT shRNA or shRNA targeting SLC38A1.

(**D**) Knockdown of GLS2 blocked serum-dependent necrosis. MEFs expressing non-targeting shRNA (NT) or two independent shRNAs targeting GLS2 were treated as indicated for 12 hrs and cell viability was subsequently measured. FBS: 5% (v/v). Western blotting (lower panel) confirmed the knockdown of GLS2 expression.
(**E**) GOT1 RNAi reduced serum-dependent necrosis. Left: MEFs expressing non-targeting (NT) shRNA or shRNA targeting GOT1 were treated as indicated for 12 hrs and cell viability was subsequently measured. Right: qPCR measurement of GOT1 mRNA levels in MEFs infected with NT shRNA or shRNA targeting GOT1.
(**F**) α-ketoglutarate can mimic the death-inducing activity of L-Gln but in a manner insensitive to the transaminase inhibitor AOA. MEFs were treated as indicated for 12 hrs, and cell viability was subsequently measured. α-KG: (Dimethyl-α-Ketoglutarate), 4 mM; AOA, 0.5 mM.
See also Figure S5

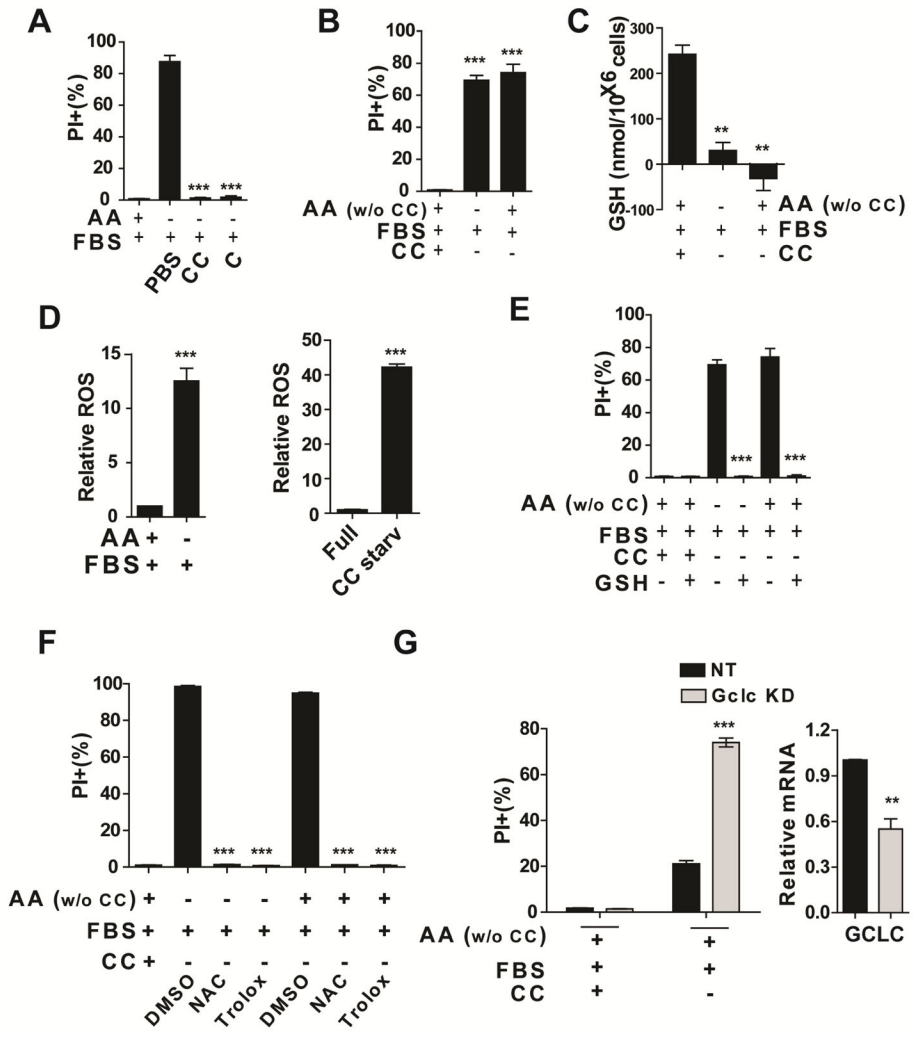

Figure 6. Cystine starvation and subsequent cellular redox homeostasis unbalance trigger serum-dependent necrosis

(**A**) Addition of cysteine (C, 0.2 mM) or cystine (CC, 0.2 mM) inhibited serum-dependent necrosis. MEFs were treated as indicated for 12 hrs. Cell death was subsequently measured by PI staining followed by flow cytometry.

(**B**) Cystine starvation alone is sufficient to induce cell death. MEFs were treated as indicated for 12 hrs and cell death was determined by PI staining coupled with flow cytometry.

(**C**) Glutathione (GSH) was depleted in the condition of serum-induced necrosis or cystine starvation. MEFs were treated as indicated for 4 hrs and harvested for total glutathione measurement.

(**D**) Accumulation of ROS in MEFs induced by serum under AA starvation condition (left) or cystine starvation (right). ROS levels in MEFs were determined by H_2DCFDA staining. H_2DCFDA assay was performed 8 hrs (Left) or 6 hours (right).

(**E**) Supplement of GSH blocked cell death induced by serum upon total AA starvation or cystine starvation. MEFs were treated as indicated for 12 hrs, and cell death was subsequently measured.

(**F**) Cell death induced by serum upon AA starvation or cystine starvation can be prevented by antioxidant reagents NAC (0.2 mM) and Trolox (0.2 mM). MEFs were treated as indicated for 12 hrs, and cell death was subsequently measured.
(**G**) GCLC RNAi sensitized serum-dependent cell death upon cystine starvation. Left: qPCR measurement of GCLC mRNA levels in MEFs infected with NT shRNA or shRNA targeting GCLC. Right: MEFs expressing non-targeting (NT) shRNA or shRNA targeting GCLC were treated as indicated for 10 hrs and cell death was subsequently measured.
See also Figure S6

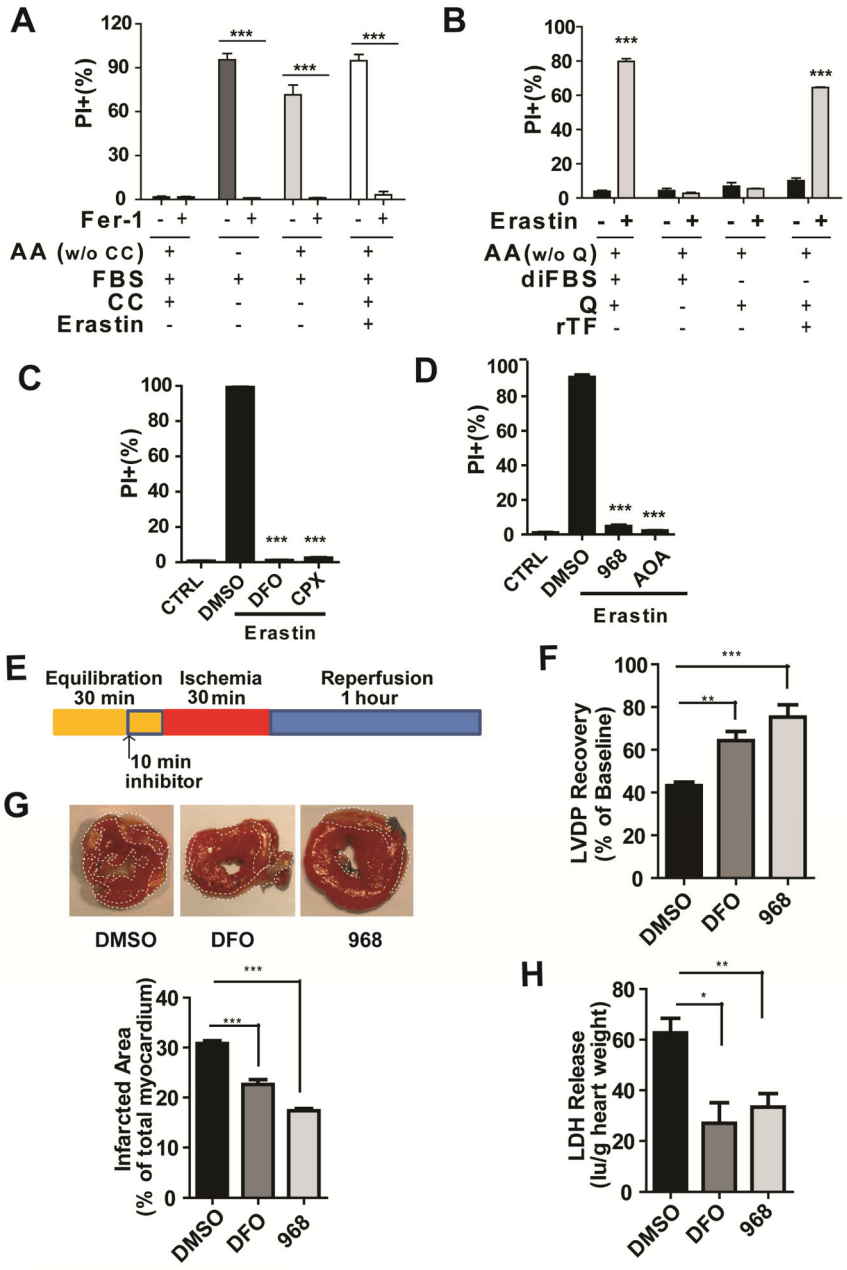

Figure 7. Serum-dependent necrosis is ferroposis and is involved in ischemia-reperfusion heart injury

(**A**) Ferroptosis inhibitor Ferrastatin-1 (Fer-1) can inhibit serum-induced necrosis upon total AA starvation or cystine (CC) starvation. MEFs were treated as indicated for 12 hrs, and cell viability was subsequently measured by PI staining followed by flow cytometry. Erastin: 1 μM.

(**B**) Erastin-induced ferroptosis required both transferrin and glutamine. *bax/bak* DKO MEFs were treated as indicated for 12 hrs, and cell death was subsequently measured by PI staining followed by flow cytometry. Erastin: 1 μM.

(**C**) Iron chelators inhibited erastin-induced ferroptosis. MEFs were treated as indicated for 12 hrs, and cell death was subsequently measured. DFO, 80 μM; CPX, 10 μM; Erastin: 1 μM.

(**D**) Inhibition of GLS by compound 968 (20 μM) or transaminases by pan-transaminases inhibitor AOA (0.5 mM) blocked erastin-induced ferroptosis. MEFs were treated as indicated for 12 hrs, and cell death was subsequently measured. Erastin, 1 μM.

(**E**) Schematic protocol for the ischemia-reperfusion study involving 30-min of global ischemia followed by a 60-min reperfusion period. (**F**) Determination of myocardial ischemic injury and function by left ventricular developed pressure (LVDP) recovery, showing improved functional recovery upon treatment with DFO or compound-968 (968). DFO: 80 μM, 968: 25 μM.

(**G**) Representative cross-sections of hearts stained with TTC, demonstrating reduced infarct injury (pale region) upon DFO or 968 treatment. The plot (lower panel) shows quantification of infarct size of each group.

(**H**) Determination of myocardial ischemic injury by lactate dehydrogenase (LDH) release, demonstrating reduced infarct injury in the hearts treated with DFO or 968.

See also Figure S7